Journal of Materials and Environmental Science
ISSN : 2028-2508
e-ISSN : 2737-890X
CODEN : JMESCN


J. Mater. Environ. Sci., 2026, Volume 17, Issue 7, Page 1190-1205

http://www.jmaterenvironsci.com

# Characterization of the Spectral Signatures of Bio-Organic Compounds Using Spectroscopic Measurements: Diurnal Variability and Multi-Method Identification in the Urban Lakes of Yamoussoukro (Côte d'Ivoire)

**Toh Kalou Chrislaire[1,2**], Yamoa Assoumou Saint-doria[1*], Bosson Jocelyne Mamaket[2], Bagui Kossan Olivier[1], Diabré Inoussa[1], Kouakou Kouakou Constant[1,2], Zoueu T. Jérémie[1]**

*1) Laboratoire d'Instrumentation, Image et Spectroscopie (L2IS), INPHB, Yamoussoukro, Côte d'Ivoire*

*2) Laboratoire de Physique Fondamentale et Appliquée (LPFA), UNA, Abidjan, Côte d'Ivoire*

**Corresponding author, Email address: saintdoriay@gmail.com*

***Corresponding author, Email address: tohchrislaire@gmail.com*

***Received*** *28 May 2026,*
***Revised*** *19 July 2026,*
***Accepted*** *21 July 2026*

***Keywords:***
- ✓ *Absorption spectroscopy;*
- ✓ *Chlorophyll-a;*
- ✓ *Urban lakes;*
- ✓ *Yamoussoukro;*
- ✓ *Spectral Angle Mapper;*
- ✓ *Pearson correlation;*
- ✓ *USB4000;*
- ✓ *Bio-organic compounds.*

***Citation****: Chrislaire T. K., Saint-Doria Y. A., Mamaket B. J., Olivier B. K., Inoussa D., Constant K. K., Jérémie Z. T. (2026) Characterization of the Spectral Signatures of Bio-Organic Compounds Using Spectroscopic Measurements: Diurnal Variability and Multi-Method Identification in the Urban Lakes of Yamoussoukro (Côte d'Ivoire), J. Mater. Environ. Sci., 17(7), 1190-1205*

**Abstract:** The urban lakes of Yamoussoukro (Côte d'Ivoire) are subjected to significant anthropogenic pressures, resulting in complex alterations in their bio-organic composition. Absorption spectroscopy represents a promising non-invasive approach for their characterization. Absorption spectra (345-800 nm) were acquired at three periods of the day (morning, noon, and evening) across 13 lakes, with three samples collected per period. Compound identification was based on a multi-method approach combining normalized Euclidean distance, Pearson correlation (raw spectra and second derivatives), spectral angle mapper (SAM), and characteristic peak detection, integrated into a normalized composite score ranging from 0 to 1. Chlorophyll-a was identified as the dominant compound in 38 out of 39 cases (97%), with composite scores of S = 0.6227 (morning) and S = 0.7496 (evening) recorded at Gare Républicaine Lake. This lake was the only site exhibiting temporal variability, with Chlorophyll-b identified at noon (S = 0.6663; r = +0.5714). Absorption bands at 430-441 nm and 663-687 nm, corresponding to the characteristic Soret and Qy bands of chlorophyll-a, were consistently detected, yielding a coincidence score of 1.00 across all three periods. The predominance of chlorophyll-a confirms intense phytoplanktonic activity in these urban water bodies, with important implications for eutrophication monitoring.

## Introduction

Lake ecosystems play a fundamental role in biogeochemical cycles and constitute vital resources for human populations (Tranvik *et al.* 2009; Bastviken *et al.*, 2011; Dashora *et al.*, 2025; Zhao *et al.*, 2025; Hounshell *et al.*, 2026). In sub-Saharan tropical environments, these ecosystems are exposed to conditions favorable to phytoplankton development, including high temperatures, intense irradiance, and nutrient availability resulting from terrestrial and anthropogenic inputs (Zohary *et al.* 2012). Bio-organic compounds, including photosynthetic pigments (chlorophylls and carotenoids) and colored dissolved organic matter

(CDOM), represent the main optical determinants of these waters and directly influence their spectral signatures within the visible range (400-800 nm).

Absorption spectroscopy constitutes a non-invasive, rapid, and cost-effective technique for the optical characterization of natural waters (Kirk 1994; Bricaud *et al.* 1995), offering a direct pathway toward applications in hyperspectral remote sensing and water quality monitoring (Dekker et al. 2002; Giardino et al. 2019). The deconvolution of absorption spectra in urban aquatic environments, where source mixtures are inherently complex, represents a major analytical challenge - one that conventional single-method approaches are often ill-equipped to address.

To date, relatively few studies have addressed the spectral characterization of urban water bodies in West Africa, where cumulative anthropogenic pressures - domestic effluent discharge, urban surface runoff, and peri-urban agricultural activities - generate distinctive eutrophic conditions characterized by chronic nutrient loading (Groga et al. 2012). The city of Yamoussoukro, the political capital of Côte d'Ivoire, with its extensive network of urban lakes, constitutes a particularly compelling study site in this regard. The identification of bio-organic compounds in such systems presents site-specific analytical challenges: spectral overlap among co-occurring pigments, potential dominance of the CDOM absorption background, and pronounced diel temporal variability driven by photosynthetic cycles and thermally induced vertical mixing processes. The absence of unambiguous visual concordance between field-measured spectra and pure-compound reference spectra precludes purely qualitative interpretation and necessitates the systematic application of complementary quantitative methodological frameworks. The primary objective of this study is to characterize the spectral signatures of bio-organic compounds across the 13 lakes of Yamoussoukro from field spectroscopic measurements and to identify their nature through a multi-method analytical approach. The specific objectives are as follows:

- to acquire absorption spectra (345-800 nm) at three distinct daily periods and at multiple sampling points per lake;
- to develop and comparatively evaluate four complementary spectral identification methods: normalized Euclidean distance, raw and second-derivative Pearson correlation, Spectral Angle Mapper (SAM), and characteristic peak detection;
- to derive a multi-method convergence composite score enabling robust and reproducible compound identification;
- to extend the analysis across all 13 lakes of the study area and to produce a spatially comprehensive inventory of identified bio-organic compounds.

Given the prevailing tropical climatic conditions and the elevated nutrient loading characterizing these urban water bodies, we hypothesize that chlorophyll-a constitutes the dominant bio-organic compound, and that a multi-method approach will yield more robust and reliable identification outcomes than any single technique applied in isolation.

## 2. Materials and Methods

### 2.1. Study Area

The study was conducted on 13 urban and peri-urban water bodies located within the city of Yamoussoukro, the political capital of Côte d'Ivoire (**Figure 1**). The regional climate is classified as tropical humid (Aw, Köppen), characterized by a dry season extending from November to March and a major rainy season from April to July, with mean annual rainfall of approximately 1,100 mm. The 13 water bodies investigated are Lake GR Gare Républicaine, Lake 13 INPHB, Lake 1 (Derrière la Mairie), Lakes 2 through 4 (Présidentiel

FHB), Lake 5 (Restaurant Brisé), Lake 6 (Moscati), Lake 8 (Rue des Maquis), Lake 9 (Hôtel Fanon), Lake 10 (EPP N'Gokro), Lake 12 (Route Didiévie), and Lake 11 (Palace Hôtel). These lakes collectively represent a gradient of anthropogenic pressure, ranging from heavily urbanized catchments receiving direct domestic and runoff inputs to more sheltered peri-urban environments.

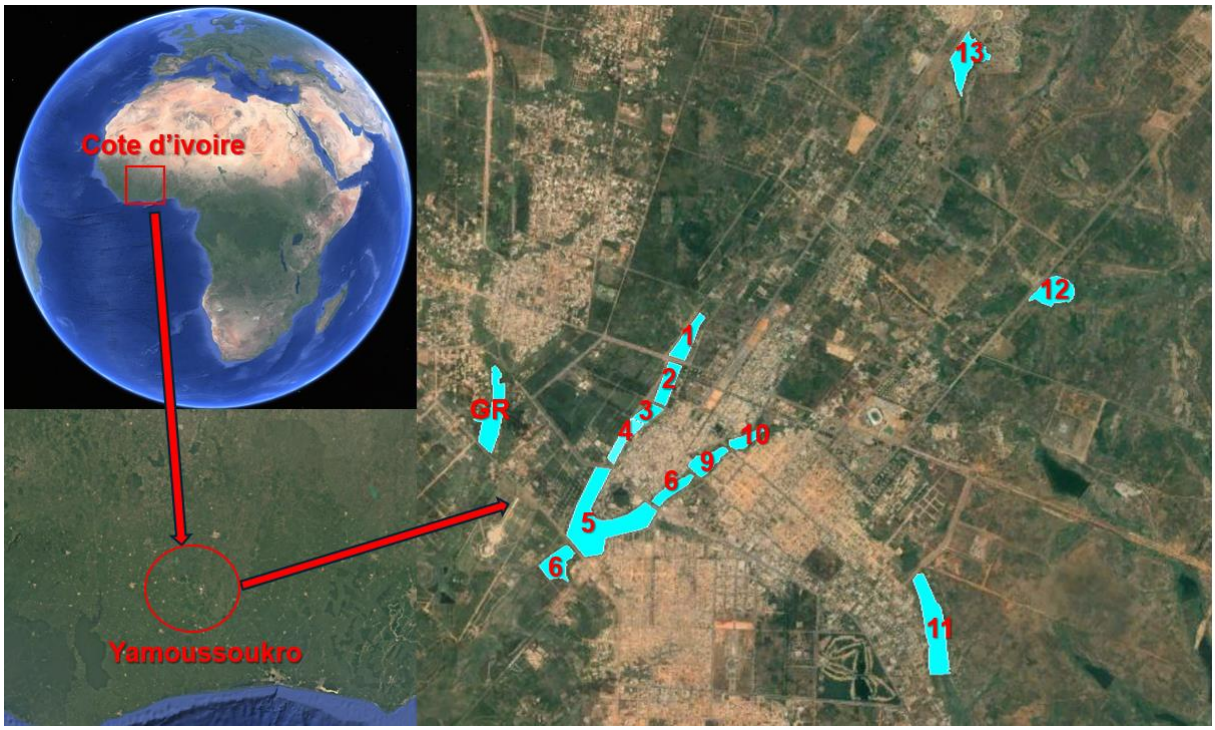


**Figure 1.** *Aerial view of the 13 sampled lakes within the city of Yamoussoukro, Côte d'Ivoire. Source: Google Earth Pro.*

## 2.2. Sampling Protocol

For each lake, three replicate samples were collected at three distinct daily periods - morning (06:00-09:00), noon (11:00-13:00), and evening (16:00-18:00) - in order to capture the diel variability of optical properties associated with photosynthetic cycles and thermally driven vertical stratification. Each sample was collected from the surface layer (0-30 cm depth) at multiple spatially distributed points within the lake, to account for intra-lake spatial heterogeneity. Samples were stored in opaque plastic bottles and analyzed as promptly as possible following collection to minimize biological degradation and photochemical alteration. 117 samples were collected across all 13 lakes and three daily periods (**Figure 2**).

## 2.3. Experimental Setup and Spectral Data Acquisition

Laboratory-based optical characterization of water samples was performed using a compact fiber-optic spectroscopy system, the components of which are illustrated in **Figure 3**. The setup comprised the following elements: (i) a broadband UV-Vis-NIR light source (Ocean Optics UV-Vis-NIR Light Source) emitting a continuous spectrum spanning the ultraviolet, visible, and near-infrared domains, directed toward the sample via an emission optical fiber; (ii) a quartz cuvette holder (Port-Cuvette) accommodating the water sample and ensuring optimal light-matter interaction over a calibrated optical path length; (iii) optical fibers guiding both the incident illumination to the sample and the transmitted or absorbed signal to the detector, thereby minimizing coupling losses; (iv) a USB4000 miniature spectrometer (Ocean Optics) measuring the transmitted or absorbed spectrum over the 345-1050 nm range at a spectral resolution of approximately 0.2-0.5 nm; and

(v) a laptop computer providing real-time data acquisition, storage, and preliminary processing via the SpectraSuite software package.


**Figure 2.** *Photographs of water samples collected from the 13 study lakes. a) Lake 13 INPHB. b) Lake 14 Palace Hôtel. c) Lake 13 Route Didiévie. d) Lake 6 Moscati. e) Lake 8 Rue des Maquis. f) Lake 9 Hôtel Fanon. g) Lake 10 EPP N'Gokro. h) Lake 5 Restaurant Brisé. i) Lake 4 Présidentiel FHB. j) Lake 3 Présidentiel FHB. k) Lake 1 Présidentiel FHB. l) Lake 2 Présidentiel FHB. m) Lake GR Gare Républicaine.*

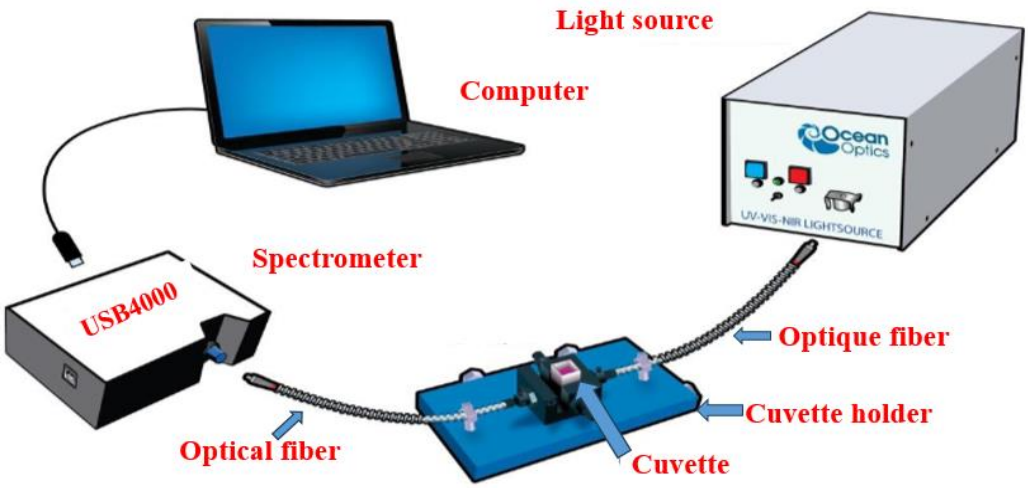


**Figure 3.** Schematic diagram of the experimental setup used for absorption spectra acquisition.

This compact and portable configuration enables the acquisition of precise spectral signatures from aquatic samples, essential for the quantification of optically active parameters such as dissolved organic matter, chlorophyll pigments, and turbidity. Spectral analysis was focused on the visible domain (350-800 nm), which encompasses the principal absorption features of the bio-organic compounds of interest.

## 2.4. Data Preprocessing

Raw spectral data were preprocessed in MATLAB through the following sequential steps:

- elimination of duplicate wavelength entries by averaging their corresponding absorbance values;

- removal of non-numeric values (NaN) and negative absorbance arising from instrumental zero-offset drift;
- interpolation onto a common wavelength grid (350-800 nm, $\Delta\lambda$ = 0.5 nm) using the pchip algorithm (piecewise cubic Hermite interpolating polynomial), which preserves local monotonicity and avoids spurious oscillations;
- computation of the mean spectrum for each daily period, together with the median, first and third quartiles (Q1, Q3), and interquartile range (IQR), to characterize inter-replicate variability;
- Savitzky-Golay smoothing (polynomial order 4, window width 10 nm = 21 points) prior to second-derivative computation, to prevent noise amplification inherent to finite-difference differentiation operators.

## 2.5. Reference Spectra

Reference spectra for the four bio-organic compounds of interest were constructed from bibliographic data and modeled as analytical functions - Gaussian functions for pigment absorption bands, and an exponential decay function for CDOM. This approach provides physically consistent spectral templates suitable for quantitative comparison with field-measured spectra. **Table 1** summarizes the characteristic absorption bands used to parameterize each reference spectrum.

**Table 1.** Reference spectra of bio-organic compounds investigated in this study.

| Compound | Characteristic peaks | Spectral range | Source |
|---|---|---|---|
| **Chlorophyll-a** | 430 nm, 675 nm | 430-460 / 650-700 nm | (Jeffrey and Humphrey 1975; Bricaud et al. 1995) |
| **Chlorophyll-b** | 460 nm, 647 nm | 430-480 / 630-660 nm | (Lichtenthaler 1987) |
| **CDOM** | Exponential decay | 300-500 nm | (Stedmon and Markager 2003) |
| **β-Carotene** | 450 nm, 480 nm | 430-500 nm | (Davies 1980) |

## 2.6. Spectral Identification Methods

### *2.6.1. Normalized Euclidean Distance (M1)*

This method consists of normalizing each measured spectrum by its maximum value (rescaling to the range [0, 1]), then interpolating the reference spectrum onto the same wavelength grid. The Euclidean norm of the point-by-point difference, divided by the total number of spectral points, yields the dissimilarity distance:

$$d = \frac{\sqrt{\sum_i \left(\hat{A}_{mes}(\lambda_i) - \hat{A}_{ref}(\lambda_i)\right)^2}}{N} \qquad (\boldsymbol{Eqn.1})$$

The compound associated with the minimum value of d is identified as the best spectral match.

Limitations: this metric is sensitive to the overall spectral shape, such that a smooth CDOM exponential background may dominate the distance and mask pigment features; it does not account for the positions of characteristic absorption peaks; and it provides no confidence threshold for discrimination.

### *2.6.2. Pearson Correlation: Raw Spectra (M2) and Second Derivatives (M2b)*

The Pearson correlation coefficient measures shape similarity between two spectral curves independently of their respective amplitudes, addressing the question: do both spectra rise and fall at

the same wavelengths? The reference spectrum is first interpolated onto the measurement wavelength grid, after which both spectra are mean-centered prior to computing the coefficient:

$$r = \frac{\sum_{i=1}^{N}\left((A_{mes})(\lambda_i) - \bar{A}_{mes}\right)\left(A_{ref}(\lambda_i) - \bar{A}_{ref}\right)}{\sqrt{\sum_i (A_{mes} - \bar{A}_{mes})^2}\,.\sqrt{\sum_i \left(A_{ref} - \bar{A}_{ref}\right)^2}} \qquad (\boldsymbol{Eqn.2})$$

The compound yielding the maximum value of r - that is, the coefficient closest to +1 - is identified as the best spectral match.

Method M2b applies the same formula to the second derivatives of the spectra, computed via a centered finite-difference scheme (step size h = 0.5 nm) following Savitzky-Golay smoothing: (SG):

$$\left.\frac{d^2A}{d\lambda^2}\right|_{\lambda_i} = \frac{A(\lambda_{i+1}) - 2A(\lambda_i) + A(\lambda_{i-1})}{h^2} \qquad (\boldsymbol{Eqn.3})$$

This transformation effectively suppresses the CDOM contribution, since the second derivative of its characteristic exponential decay satisfies ($d^2e^{-s\lambda}/d\lambda^2 = S^2e^{-s\lambda} \approx 0$ for S = 0,015 $nm^{-1}$, yielding a value of approximately ≈ 0,000225 - negligibly small). As a result, the smooth CDOM background is flattened in the second-derivative space, allowing the narrow absorption peaks of photosynthetic pigments to emerge with greater spectral contrast. Prior Savitzky-Golay smoothing is essential in this context, as the finite-difference operator amplifies high-frequency noise by a factor of $1/h^2$.

***2.6.3. Spectral Angle Mapper (SAM, M3)***

In this approach, each spectrum is treated as a vector in an N-dimensional space, where N denotes the number of spectral channels. The SAM computes the angle between the measured spectral vector and each reference vector; the smaller the angle, the greater the shape similarity between the two spectra:

$$\theta = arcos\left(\frac{\vec{A}_{mes}.\vec{A}_{ref}}{\|\vec{A}_{mes}\|.\|\vec{A}_{ref}\|}\right) \epsilon \left[0,\ \frac{\pi}{2}\right] radians \qquad (\boldsymbol{Eqn.4})$$

The compound associated with the minimum angle θ is identified as the best spectral match.

A key property of the SAM is its amplitude invariance: division by the respective Euclidean norms of both vectors cancels any scaling effect, such that a spectrum twice as intense as the reference will yield an identical angle θ. This makes the method particularly well-suited to aquatic environments where absolute absorption magnitudes vary substantially among samples due to differences in biomass concentration or optical path length.

***6.4. Characteristic Peak Detection (M4)***

Local maxima of the smoothed spectra are detected using two criteria: a minimum prominence of 5% of the spectral maximum, and a minimum inter-peak separation of 20 nm. For each reference absorption band $b_k$ of a given compound, the minimum distance to the set of detected peaks is computed, and a coincidence is recorded if this distance falls within a tolerance of ±15 nm:

$$d(b_k) = \min_{p \in peaks} \left|\lambda_{peak}(p) - b_k\right| \qquad (\boldsymbol{Eqn.5})$$

$$coincidence(b_k) = \begin{cases} 1 & si\ d(b_k) \leq 15\ nm \\ 0 & otherwise \end{cases}$$

All coincidences are summed and divided by the total number of reference bands for that compound, yielding a normalized concordance score:

$$score(\text{Compound}) = \frac{\sum_{k=1}^{N_{bands}} coincidence(b_k)}{N_{bands}} \quad (\boldsymbol{Eqn.6})$$

The identified compound is that which maximizes this score:

$$Identified\ (compound) = arg \max_{compound}[score(compound)] \quad (\boldsymbol{Eqn.7})$$

A score of 1.00 indicates perfect coincidence between all detected peaks and the reference absorption bands of the candidate compound, while a score of 0.00 indicates the complete absence of any matching peak within the prescribed tolerance window.

#### *2.6.5. Multi-Method Convergence Composite Score*

To synthesize the outputs of all five approaches into a single, robust identification criterion, the individual scores are first normalized to the interval [0, 1]. For distance- and angle-based metrics - where smaller values indicate greater similarity - the normalization is inverted so that a perfect match consistently yields a score of 1. The five normalized scores are then averaged to produce the composite score:

$$S_{composite} = \frac{S_{dist} + S_{pearson} + S_{D2} + S_{SAM} + S_{Peaks}}{5} \quad (\boldsymbol{Eqn.8})$$

where each component is defined as:

$$S_{dist} = 1 - \frac{d - d_{min}}{d_{max} - d_{min}}, \quad S_{Pearson} = \frac{r+1}{2}, \quad S_{D2} = \frac{r_{D2}+1}{2}, \quad S_{SAM} = 1 - \frac{\theta}{\frac{\pi}{2}}, \quad S_{peaks} = score\ (\boldsymbol{Eqn.6})$$

The compound yielding the maximum value of $S_{composite}$ is retained as the identified bio-organic compound. This convergence-based approach mitigates the individual limitations of each method: ambiguities arising from CDOM background dominance, amplitude sensitivity, or noise-induced artifacts are collectively attenuated when multiple independent lines of spectral evidence point consistently toward the same compound.

## 3. Results

### 3.1. Raw Spectral Characteristics: Lac Gare Républicaine (Test Case)

The absorption spectra of the nine samples collected at Lac Gare Républicaine (**Figures 4a–c**) exhibit strong absorption in the blue region (400-500 nm) and well-defined spectral structures in the red (630-700 nm), both characteristic of photosynthetic pigments. Moderate inter-replicate variability is observed in the blue region, reflecting spatial heterogeneities in phytoplankton biomass distribution across the lake surface. Importantly, the observed spectral signatures depart substantially from those classically reported in the literature for pure compounds (**Figure 5**), underscoring the inherent complexity of mixed-source optical signals in urban aquatic environments - a complexity that precludes reliable compound identification through visual inspection alone and motivates the multi-method quantitative framework developed in this study. Mean spectra for each daily period, together with their corresponding IQR envelopes and medians, are presented in **Figure 6**. This analysis

confirms the relative stability of spectral signatures among replicates within each period, while revealing subtle yet consistent inter-period differences, particularly in the red region (630-700 nm), attributable to diel fluctuations in phytoplankton biomass concentration.

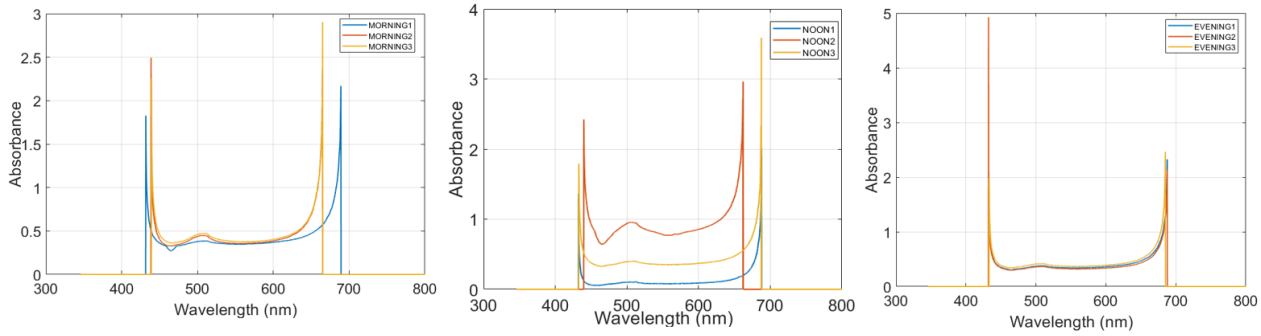


**Figure 4a–c.** Individual absorption spectra acquired at Lac Gare Républicaine across the three daily sampling periods: morning, noon, and evening (three replicates per period). Spectral variability among replicates reflects spatial heterogeneity in phytoplankton biomass within the lake.

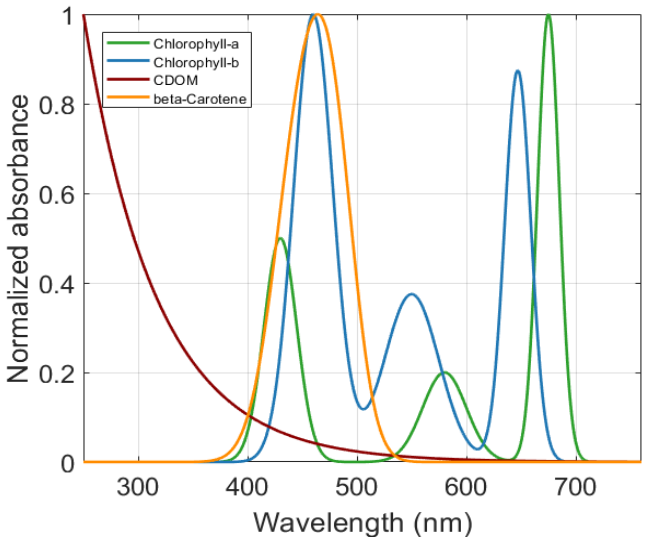


**Figure 5.** Reference absorption spectra of the four bio-organic compounds considered in this study: chlorophyll-a (Chl-a), chlorophyll-b (Chl-b), colored dissolved organic matter (CDOM), and β-carotene.

The normalized Euclidean distance results (**Table 2**) indicate a predominance of chlorophyll-b in the morning and at noon, as evidenced by the lowest dissimilarity distances recorded for that compound ($d = 0.0084$ and $d = 0.0085$, respectively). In the evening, however, chlorophyll-a emerges as the dominant compound, yielding the minimum observed distance ($d = 0.0070$), reflecting a markedly improved spectral correspondence between field measurements and the chlorophyll-a reference spectrum during this period. **Table 3** presents the Pearson correlation coefficients computed between the mean measured spectra and the four reference spectra. Chlorophyll-b yields the highest correlations in the morning ($r = +0.5714$) and at noon ($r = +0.5547$), while chlorophyll-a is the best-correlated compound in the evening ($r = +0.5169$). CDOM displays negative correlations across all three periods ($r \in [-0.47; -0.50]$), indicating a pronounced spectral shape dissimilarity with the measured spectra and effectively ruling it out as a dominant contributor.

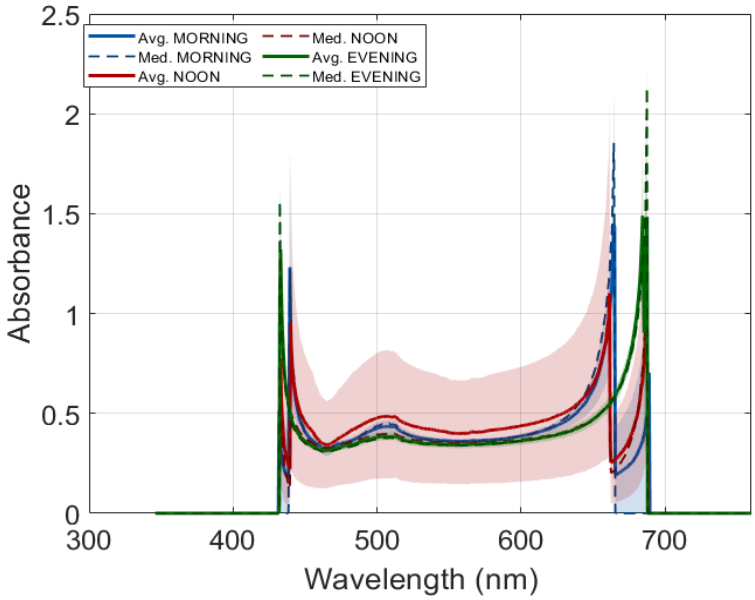


**Figure 6.** Mean absorption spectra per daily period (morning, noon, evening) with IQR envelope and median: Lac Gare Républicaine.

**Table 2.** Bio-organic compound identification by normalized Euclidean distance (Lac Gare Républicaine).

| Period | Chlorophyll-a | Chlorophyll-b | CDOM | β-carotene | Best identified compound |
|---|---|---|---|---|---|
| Morning | 0,0091 | 0,0084* | 0,0086 | 0,0116 | Chlorophyll-b (d = 0,0084) |
| Noon | 0,0104 | 0,0085* | 0,0110 | 0,0124 | Chlorophyll-b (d = 0,0085) |
| Evening | 0,0070* | 0,0097 | 0,0087 | 0,0119 | Chlorophyll-a (d = 0,0070) |

*Asterisks (*) denote the minimum distance value per period.*

**Table 3.** Pearson correlation coefficients between mean measured spectra and reference spectra (raw spectra).

| Period | Chl-a | Chl-b | CDOM | β-Carotene | Best compound |
|---|---|---|---|---|---|
| Morning | +0,1192 | **+0,5714** | −0,4680 | +0,1516 | Chlorophylle-b |
| Noon | +0,1417 | **+0,5547** | −0,5023 | +0,1578 | Chlorophylle-b |
| Evening | **+0,5169** | +0,3682 | −0,4490 | +0,1175 | Chlorophylle-a |

*Bold values indicate the maximum coefficient per period (decision criterion: r closest to +1).*

Second-derivative analysis (**Table 4**) allows the limitations associated with CDOM background dominance to be overcome. Although the resulting coefficients are inherently low in absolute magnitude ($r < 0.03$) - reflecting the complexity of fine spectral structures in natural aquatic matrices - this approach independently confirms chlorophyll-a as the best match in the evening, chlorophyll-b at noon, and suggests a spectral affinity with β-carotene in the morning, consistent with the known absorption features of accessory carotenoid pigments in that spectral region.

**Tableau 4.** Pearson correlation coefficients computed on second-derivative spectra (D2).

| Period | Chl-a | Chl-b | CDOM | β-Carotene | Best compound |
|---|---|---|---|---|---|
| Morning | −0,0352 | −0,0042 | +0,0004 | **+0,0014** | β-Carotène |
| Noon | −0,0155 | **+0,0068** | +0,0005 | +0,0016 | Chlorophylle-b |
| Evening | **+0,0202** | −0,0025 | +0,0004 | +0,0019 | Chlorophylle-a |

*Bold values indicate the maximum coefficient per period.*

The SAM results corroborate the trends established by the preceding methods. Minimum spectral angles are obtained with chlorophyll-b in the morning ($\theta = 0.6936$ rad = 39.74°) and at noon ($\theta = 0.7021$ rad = 40.23°), and with chlorophyll-a in the evening ($\theta = 0.8156$ rad = 46.73°). CDOM

consistently yields the largest angles across all periods (θ ≈ 1.39-1.40 rad ≈ 80°), confirming its pronounced spectral dissimilarity with the measured spectra and further excluding it as a dominant contributor to the observed optical signatures. These findings are fully consistent with those of the distance- and correlation-based approaches, reinforcing the convergent identification of chlorophyll-b as the dominant compound during morning and noon periods, and chlorophyll-a in the evening (**Figure 7**).

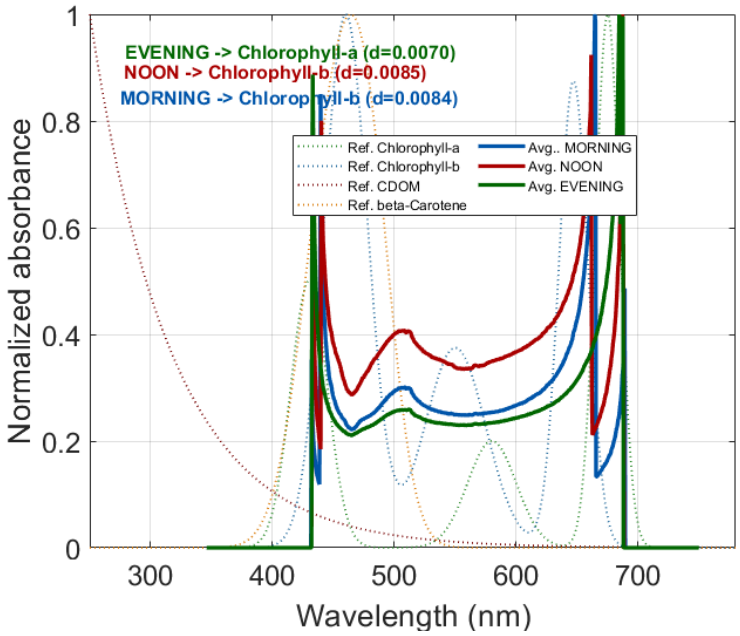


**Figure 7.** Comparison of mean measured spectra with bio-organic compound reference spectra, illustrated through the Spectral Angle Mapper (SAM) approach. Angular separation between measured and reference vectors reflects spectral dissimilarity; minimum angles indicate the best-matching compound per period.

Automated local maxima detection (**Table 5** and **Figure 8**) identifies four absorption peaks in the morning spectra (441.0, 506.5, 663.0, and 687.0 nm), four at noon (442.0, 506.0, 659.5, and 686.0 nm), and two in the evening (434.5 and 685.0 nm). Coincidence with the reference absorption bands of chlorophyll-a (430 nm and 675 nm, ±15 nm tolerance) is perfect across all three daily periods, yielding a concordance score of 1.00 in each case. Conversely, CDOM obtains a score of 0.00 for all periods, as its reference bands (300 and 350 nm) fall entirely outside the spectral range of detected peaks, providing unambiguous negative evidence for its optical dominance. These results constitute the strongest single-method discriminating signal in the dataset, unequivocally identifying chlorophyll-a as the compound whose absorption features are most faithfully reproduced in the measured spectra.

**Tableau 5.** Characteristic peak detection results and concordance scores for each daily period and each candidate compound.

| Period | Detected peaks (nm) | Chl-a [430,675] | Chl-b [460,647] | CDOM [300,350] | β-Car [450,480] |
|---|---|---|---|---|---|
| Morning | 441,0 ; 506,5 ; 663,0 ; 687,0 | **Score=1,00 ✓✓** | Score=0,00 ✗✗ | Score=0,00 ✗✗ | Score=0,50 ✓✗ |
| Noon | 442,0 ; 506,0 ; 659,5 ; 686,0 | **Score=1,00 ✓✓** | Score=0,50 ✗✓ | Score=0,00 ✗✗ | Score=0,50 ✓✗ |
| Evening | 434,5 ; 685,0 | **Score=1,00 ✓✓** | Score=0,00 ✗✗ | Score=0,00 ✗✗ | Score=0,00 ✗✗ |

*✓: coincident band within ±15 nm tolerance; ✗: band absent or outside tolerance window.*

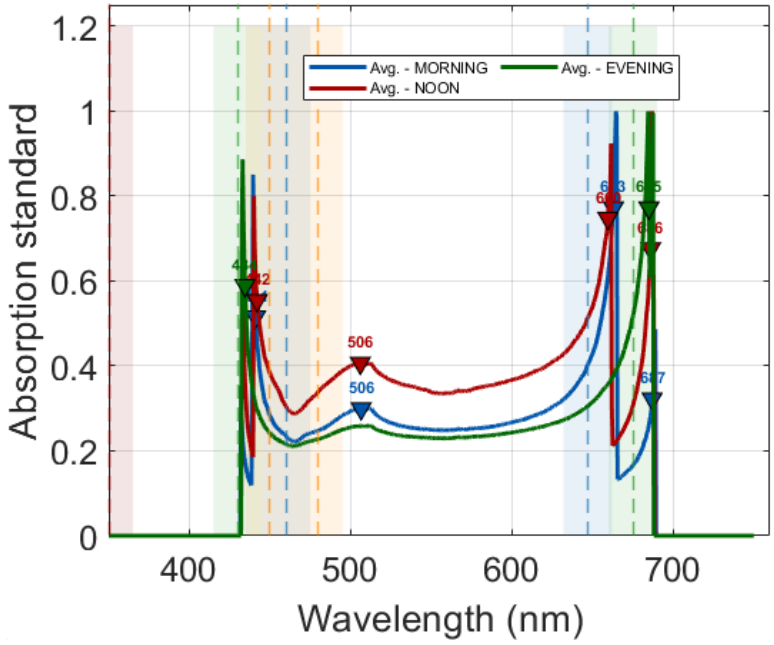


**Figure 8.** Automated detection of characteristic absorption peaks and correspondence with reference bands of candidate compounds across morning, noon, and evening periods.

**Table 6** consolidates the composite convergence scores across all five methods. Chlorophyll-a achieves the highest composite score in the morning (S = 0.6227) and evening (S = 0.7496), while chlorophyll-b dominates at noon (S = 0.6663). All three leading scores exceed the indicative convergence threshold of 0.5, above which multi-method agreement is considered sufficiently robust to support compound identification. CDOM and β-carotene consistently yield composite scores below 0.40 across all periods, confirming their negligible contribution to the dominant optical signature of the lake at the time of sampling (**Figure 9**).

**Tableau 6.** Multi-method convergence composite scores for each daily period and each candidate compound, Lac Gare Républicaine. The identified compound per period corresponds to the maximum composite score.

| Period | Chl-a | Chl-b | CDOM | β-Carotene | Identified compound |
|---|---|---|---|---|---|
| Morning | **0,6227** | 0,5680 | 0,3312 | 0,3751 | Chlorophylle-a |
| Noon | 0,5770 | **0,6663** | 0,2289 | 0,3773 | Chlorophylle-b |
| Evening | **0,7496** | 0,4164 | 0,2882 | 0,2682 | Chlorophylle-a |

*S = (Euclidean dist. + Pearson + Pearson D2 + SAM + Peak detection) / 5, normalized to [0, 1].*

The same analytical framework was subsequently applied to the remaining 13 lakes (**Table 7**). The results reveal a striking degree of spatial homogeneity: chlorophyll-a is identified as the dominant bio-organic compound in 38 out of 39 cases (97.4%), with 12 of the 13 lakes exhibiting this pigment exclusively across all three daily periods. Lac Gare Républicaine constitutes the sole exception, displaying temporal variability characterized by the transient emergence of chlorophyll-b as the dominant compound at noon - a pattern not observed in any other lake within the study area.

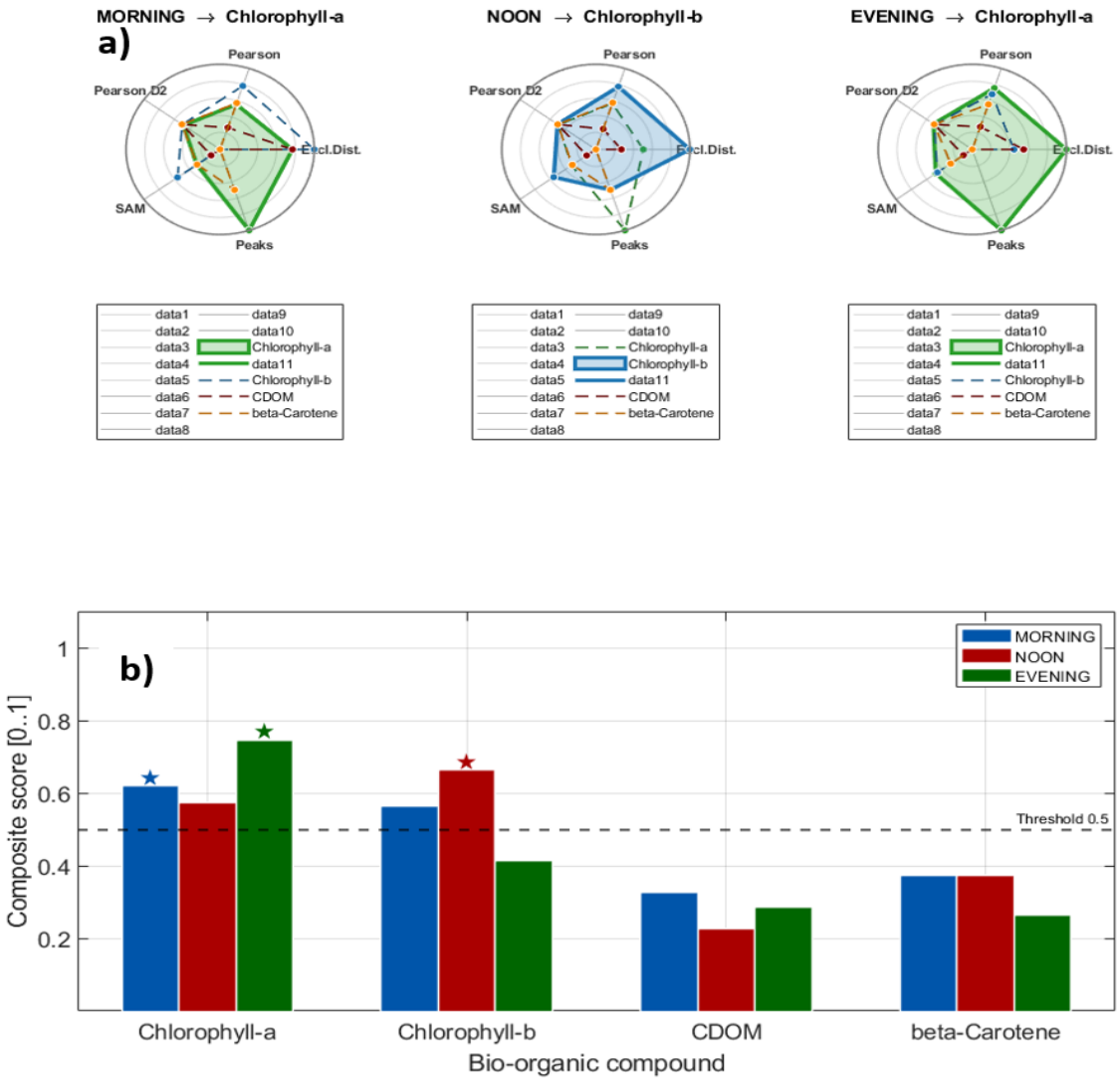


**Figue 9.** Multi-method analysis of bio-organic compound identification at Lac Gare Républicaine. (a) Radar plots illustrating the degree of convergence among the five spectral identification methods (Euclidean distance, raw Pearson correlation, second-derivative Pearson correlation, SAM, and characteristic peak detection) for each daily measurement period. (b) Normalized composite scores for each candidate bio-organic compound (chlorophyll-a, chlorophyll-b, CDOM, and β-carotene) across morning, noon, and evening periods, with indication of the compound identified by multi-method convergence.

## Discussion

The predominance of chlorophyll-a across 97% of identifications is fully consistent with the optical and biological characteristics of tropical eutrophic environments. The detected absorption bands (430–441 nm and 663–687 nm) correspond to the Soret and Qy bands of chlorophyll-a, universally documented in the literature (Jeffrey and Humphrey 1975; Bricaud et al. 1995). The slight dispersion in peak positions (±7 nm around reference values) is attributable to solvent matrix effects on the electronic structure of the pigment in natural aqueous media. The convergence of all four methods toward this compound - most notably the perfect concordance score obtained by characteristic peak detection (score = 1.00 across all three daily periods) - confirms the robustness and reliability of the identification.

**Tableau 7.** Summary of bio-organic compounds identified across the 13 lakes of Yamoussoukro by daily period and multi-method composite score.

| Lake | Morning | Noon | Evening | Identified compounds | N |
|---|---|---|---|---|---|
| LAC GARE REPUBLICAINE | Chl-a | Chl-b | Chl-a | Chl-a + Chl-b | **2** |
| LAC INPHB | Chl-a | Chl-a | Chl-a | Chl-a | 1 |
| LAC1 DERRIER LA MAIRIE | Chl-a | Chl-a | Chl-a | Chl-a | 1 |
| LAC2 PRESIDENTIEL FHB | Chl-a | Chl-a | Chl-a | Chl-a | 1 |
| LAC3 PRESIDENTIEL FHB | Chl-a | Chl-a | Chl-a | Chl-a | 1 |
| LAC4 PRESIDENTIEL FHB | Chl-a | Chl-a | Chl-a | Chl-a | 1 |
| LAC5 RESTAURANT BRISE | Chl-a | Chl-a | Chl-a | Chl-a | 1 |
| LAC6 MOSCATI | Chl-a | Chl-a | Chl-a | Chl-a | 1 |
| LAC8 RUE DES MAQUIS | Chl-a | Chl-a | Chl-a | Chl-a | 1 |
| LAC9 HOTEL FANON | Chl-a | Chl-a | Chl-a | Chl-a | 1 |
| LAC10 EPP N'GOKRO | Chl-a | Chl-a | Chl-a | Chl-a | 1 |
| LAC13 ROUTE DIDIEVIE | Chl-a | Chl-a | Chl-a | Chl-a | 1 |
| LAC14 PALACE HOTEL | Chl-a | Chl-a | Chl-a | Chl-a | 1 |

The temporal variability observed at Lac Gare Républicaine - chlorophyll-b at noon ($r = +0.5714$, $\theta = 0.7021$ rad) versus chlorophyll-a in the morning and evening - can be attributed to several interacting mechanisms. Diel variations in solar irradiance modify the pigment composition of microalgae through photoacclimation: under high irradiance conditions at noon, certain species redistribute their light-harvesting pigments to prevent photoinhibition (Falkowski and Raven 2013). Thermally driven vertical mixing processes during diurnal warming may additionally bring compositionally distinct phytoplankton assemblages to the surface at different times of day. The absence of any analogous temporal variability in the remaining 12 lakes suggests a more stable dominance of a single phytoplankton assemblage in those systems, less sensitive to diel irradiance-driven pigment reorganization.

Morning (Chlorophyll-a, $S = 0.6227$). The partial methodological convergence toward chlorophyll-a in the morning is consistent with incipient photosynthetic activity at low solar elevation angles. The slight divergence of the second-derivative method - which nominally suggests β-carotene ($r = +0.0014$) - is explained by the extremely low correlation coefficients inherent to fine spectral structure analysis in natural samples, which preclude reliable discrimination at this level. Characteristic peak detection (score = 1.00 for Chl-a) constitutes the most discriminating and reliable indicator during this period.

Noon (Chlorophyll-b, $S = 0.6663$). The identification of chlorophyll-b as the dominant compound at noon at Lac Gare Républicaine represents an original finding of this study, supported by convergent evidence from Pearson correlation ($r = +0.5547$) and the SAM ($\theta = 0.7021$ rad). This observation is consistent with the selective proliferation of green algae (Chlorophyta) - for which chlorophyll-b is

the principal accessory pigment - under the intense irradiance conditions prevailing at solar noon, as reported in photoacclimation studies of freshwater phytoplankton communities.

Evening (Chlorophyll-a, S = 0.7496). The strongest methodological convergence of the study is recorded in the evening, with the highest composite score obtained across all lakes and periods. This result is consistent with the well-documented accumulation of phytoplankton biomass at the water surface during the late afternoon, following a full day of intensive photosynthetic carbon fixation and buoyancy-regulated vertical migration.

Methodological limitations. Despite the robustness of the multi-method framework, several limitations warrant explicit consideration. First, the reference spectra employed rely on simplified analytical models - Gaussian functions for pigments and exponential decay for CDOM - derived from bibliographic data. Although these templates faithfully reproduce the principal known absorption features, they constitute an approximation of spectra measured under in situ conditions, where pigment–CDOM–particle interactions can alter optical signatures in ways not captured by idealized functions. Future integration of experimentally measured reference spectra, obtained through HPLC-based pigment analysis, would substantially improve identification precision.

Second, the sampling protocol relied on a limited number of replicates per period per lake (n = 3), which may lead to underestimation of intra-lake spatial variability. Local gradients in turbidity, water depth, and phytoplankton concentration can influence observed spectral signatures in ways not captured by sparse spatial sampling. Increasing the number of sampling points and achieving more systematic spatial coverage within each lake would enhance the representativeness of the dataset.

Third, despite Savitzky-Golay smoothing, residual high-frequency spectral noise remains capable of affecting second-derivative and peak detection analyses, potentially generating spurious local extrema. Complementary preprocessing strategies - including median filtering or adaptive noise reduction - could further improve signal quality prior to these computationally sensitive operations.

Fourth, the multi-method composite score currently assigns equal weight to all five identification approaches. Since certain methods are intrinsically, more robust for specific spectral contexts - second derivatives for chlorophyllic pigments, SAM for global shape matching - a differentiated weighting scheme calibrated to method-specific reliability and predictive performance would refine and optimize the convergence framework.

Finally, compound identification in this study rests exclusively on spectroscopic criteria, without direct taxonomic validation of the organisms present in the samples. The absence of complementary biological analyses constrains the ecological interpretation of the results. Future coupling of spectral measurements with algological microscopy or environmental DNA (eDNA) sequencing would confirm the actual presence of the phytoplankton functional groups associated with the identified spectral signatures.

Broader implications. The predominance of chlorophyll-a across all 13 lakes of Yamoussoukro constitutes strong evidence of intense and widespread phytoplankton activity, sustained by chronic nitrogen and phosphorus loading from urban surface runoff and domestic effluent discharge. These findings support the development of optical spectroscopy-based water quality monitoring tools tailored to tropical urban lakes. In the longer term, integration into autonomous sensor networks

deployed directly on the lakes would enable real-time tracking of phytoplankton dynamics and early warning of potentially harmful algal bloom events. Coupling with airborne or satellite hyperspectral remote sensing data represents a particularly promising operational perspective for large-scale, continuous monitoring of these ecologically sensitive urban water bodies.

## Conclusion

This study successfully characterized the spectral signatures of bio-organic compounds in 13 urban lakes of Yamoussoukro through laboratory spectrophotometric measurements (USB4000 spectrometer, 345–800 nm). An original multi-method analytical framework - combining normalized Euclidean distance, Pearson correlation applied to both raw spectra and second derivatives, Spectral Angle Mapper, and characteristic peak detection - was developed and synthesized into a multi-method convergence composite score. The principal findings are as follows:

- Chlorophyll-a dominates 97% of identifications (38 out of 39 cases), with composite scores confirming its predominance in the morning (S = 0.6227) and evening (S = 0.7496) at Lac Gare Républicaine;
- Absorption bands are systematically detected at 430–441 nm (Soret band) and 663–687 nm (Qy band), with a perfect peak coincidence score of 1.00 across all three daily periods;
- A unique pattern of diel temporal variability is observed exclusively at Lac Gare Républicaine, where chlorophyll-b emerges as the dominant compound at noon (S = 0.6663; r = +0.5714; $\theta$ = 0.7021 rad), most likely attributable to photoacclimation-driven pigment redistribution under peak solar irradiance;
- Strong spatial homogeneity is observed across the study area, with 12 out of 13 lakes exhibiting chlorophyll-a exclusively across all sampling periods, providing compelling evidence of widespread and intense phytoplankton activity throughout the lake network.

The multi-method convergence approach substantially reduces the identification ambiguities inherent to any single technique and constitutes a methodologically transferable framework applicable to a broad range of optically complex aquatic environments. In the short term, HPLC-based pigment analyses and microscopic taxonomic observations will provide the biological ground-truth necessary for fine-scale taxonomic identification of the dominant phytoplankton groups. In the medium term, extension of the monitoring campaign across all hydrological seasons and integration into autonomous sensor networks deployed on the lakes will lay the foundation for a sustainable, continuous water quality observation system for the urban lakes of Yamoussoukro.

**Acknowledgement:** The authors wish to thank the technical teams who participated in the field sampling campaigns, as well as the local authorities who facilitated access to the lakes of Yamoussoukro. Sentinel-2 imagery was freely accessed through the Google Earth Engine cloud-computing platform. All laboratory analyses were conducted at the Laboratory of Instrumentation, Imaging and Spectroscopy (L2IS), Institut National Polytechnique Félix Houphouët-Boigny (INPHB), Yamoussoukro, Côte d'Ivoire.

## Disclosure statement

*Conflict of Interest:* The authors declare that they have no known competing financial interests or personal relationships that could have appeared to influence the work reported in this paper.

*Compliance with Ethical Standards:* This article does not involve any studies with human participants or animals performed by any of the authors.

## References


Bastviken D, Tranvik LJ, Downing JA, et al (2011) Freshwater Methane Emissions Offset the Continental Carbon Sink. *Science* 331, 50–50. https://doi.org/10.1126/science.1196808

Bricaud A, Babin M, Morel A, Claustre H (1995) Variability in the chlorophyll-specific absorption coefficients of natural phytoplankton: Analysis and parameterization. *J Geophys Res* 100, 13321–13332. https://doi.org/10.1029/95JC00463

Dashora, M., Kumar, M., Kaushik, G. *et al.* (2025). Exploring biogeochemical transformation in a hypertrophic lake with dual focus on environmental cues and potential functional fingerprints of littoral bacteria. Sci Rep 15, 31115, https://doi.org/10.1038/s41598-025-16527-y

Davies BH (1980) Carotenoid biosynthesis. *Pigments in plants* 31–56

Dekker AG, Vos RJ, Peters SWM (2002) Analytical algorithms for lake water TSM estimation for retrospective analyses of TM and SPOT sensor data. *International Journal of Remote Sensing* 23:15–35. https://doi.org/10.1080/01431160010006917

Falkowski PG, Raven JA (2013) Aquatic photosynthesis. Princeton University Press

Giardino C, Brando VE, Gege P, et al (2019) Imaging Spectrometry of Inland and Coastal Waters: State of the Art, Achievements and Perspectives. *Surv Geophys* 40:401–429. https://doi.org/10.1007/s10712-018-9476-0

Groga N, Ouattara A, Costa SD, et al (2012) Water quality and water-use conflicts in Lake Taabo (Ivory Coast). OJE 02:38–47. https://doi.org/10.4236/oje.2012.21005

Jeffrey S t, Humphrey GF (1975) New spectrophotometric equations for determining chlorophylls a, b, c1 and c2 in higher plants, algae and natural phytoplankton. *Biochemie und physiologie der pflanzen* 167:191–194

Hounshell, A.G., Lewis, A.S.L., Howard, D.W. *et al.* (2026). Dissolved organic carbon dynamics are driven by water temperature, primary production, and anoxia over 5 years of whole-ecosystem experiments in a eutrophic reservoir. *Aquat Sci* 88, 23, https://doi.org/10.1007/s00027-025-01252-5

Kirk JT (1994) Light and photosynthesis in aquatic ecosystems. Cambridge university press

Lichtenthaler HK (1987) [34] Chlorophylls and carotenoids: pigments of photosynthetic biomembranes. In: Methods in enzymology. Elsevier, pp 350–382

Stedmon CA, Markager S (2003) Behaviour of the optical properties of coloured dissolved organic matter under conservative mixing. *Estuarine, Coastal and Shelf Science* 57:973–979

Tranvik LJ, Downing JA, Cotner JB, et al (2009) Lakes and reservoirs as regulators of carbon cycling and climate. *Limnology & Oceanography* 54:2298–2314. https://doi.org/10.4319/lo.2009.54.6_part_2.2298

Zhao Z., Wie F., Wu H., Yang M., Jin X., Wang P., Wang Q. (2025). A framework to comprehensively assess lake health from a perspective of ecosystem integrity and services, *Ecological Indicators*, 171, 113169, ISSN 1470-160X, https://doi.org/10.1016/j.ecolind.2025.113169

Zohary T, Nishri A, Sukenik A (2012) Present–absent: a chronicle of the dinoflagellate Peridinium gatunense from Lake Kinneret. In: Salmaso N, Naselli-Flores L, Cerasino L, et al. (eds) Phytoplankton responses to human impacts at different scales. Springer Netherlands, Dordrecht, pp 161–174